Supporting Information of "Conformational Transition of Poly(*N*-isopropylacrylamide) Single Chains in its Cononsolvency Process: a Study by Fluorescence Correlation Spectroscopy and Scaling Analysis"

Fei Wang,[1] Yi Shi,[1] Shuangjiang Luo,[1] Yongming Chen, Jiang Zhao[*]

Beijing National Laboratory for Molecular Sciences, Institute of Chemistry, Chinese Academy of Sciences, Beijing 100190, China

1. Materials

N-Isopropylacrylamide (NIPAM; 99%, Across) was recrystallized three times from n-hexane prior to use. The chain transfer agent (CTA), *S*-1-ethyl-*S*'-(α'-dimethyl-α''-acetic acid)trithiocarbonate, was synthesized as described in the reference[1]. 4,4'-Azobis(4-cyanovaleric acid) (V-501; 98%, Fluka), methacryloxyethyl thiocarbamoyl rhodamine B (RB-MA; Polysciences), lissamine rhodamine B ethylenediamine (SulfoRB-NH_2; Invitrogen), *N*-hydroxysuccinimide (NHS; 98%, Lancaster), *N*,*N*'-dicyclohexylcarbodiimide (DCC; Sheshan Chemicals), sodium perchlorate monohydrate (99.0%, Fluka), polystyrene gel bead (S-X1, Bio-Beads), rhodamine 6G (R6G; Standard purity, Fluka) and rhodamine B (RB, Sigma) were used as received without further treatment. Methanol, ethanol, *N*,*N*-dimethylformamide (DMF) and triethylamine (Et_3N), all from Beijing Chemical Reagent Co., were distilled prior to use. Coverslips (0.16 mm thick) were purchased from Fisherbrand. Deionized water (18.2 MΩ·cm^{-1}) was obtained by Millipore. Ultrafiltration tubes with the molar weight cutoff (MWCO) of 5 000 g·mol^{-1} and 10 000 g·mol^{-1} were purchased from Sartorius. Dialysis membrane bags with MWCO of 3 500 g·mol^{-1} and 7 000 g·mol^{-1} were purchased from Viskase. Other reagents were commercially available and used as received.

[1] Also affiliated with Graduate University of Chinese Academy of Sciences.

[*] Corresponding author: jzhao@iccas.ac.cn.

2. Preparation and characterization of fluorescently labeled PNIPAMs

2.1 RAFT synthesis of PNIPAM (N=190, 290 and 680) with the labeling by copolymerization

The radical addition-fragmentation chain transfer (RAFT) polymerization (see Approach 1 of Scheme 1 in text) was adopted with varied feed ratios to prepare PNIPAM with varied lengths (see SI-Table). The carboxyl-containing trithiocarbonate used is a highly efficient CTA in previous studies.[2] A typical procedure for the RAFT synthesis of PNIPAM was as follows. A glass ampoule was charged with CTA, V-501, NIPAM (1.0 g, 3.0 mol·L^{-1}) and 2.9 mL reaction medium (DMF or methanol). A proportion of fluorescent comonomer RB-MA was added into the feeding stock. The mixture was degassed under reduced pressure by three freeze-pump-thaw cycles with liquid nitrogen. The polymerization was carried out with vigorous stirring under argon atmosphere for varied hours. The RAFT polymerization was terminated by freezing the ampoule with liquid nitrogen. The reaction solution was diluted with DMF and then precipitated into anhydrous diethyl ether in excess twice. The solids were collected by centrifugation and dried overnight in a vacuum oven at room temperature, and were characterized.

Table-S1. Parameters for RAFT, characterization results and fluorescence labeling.

No.	[NIPAM]: [CTA]: [V-501]: [RB –MA]	RAFT conditions (a)	Conv./% (b)	$N_n/10^2$ (c)	PDI (d)	$N/10^2$ (c)	Labeling (e)
PNIPAM-86	100: 1: 0.1: 0	3.5 h, in DMF, 65℃	74	0.74	1.17	0.86	End-capping
PNIPAM-190	200: 1: 1/3: 1	17 h, in DMF, 65℃	87	1.7	1.10	1.9	Copolym.
PNIPAM-290	320: 1: 1/3: 1	16 h, in DMF, 65℃	85	2.7	1.07	2.9	Copolym.
PNIPAM-680	710: 1: 1/3: 1	16 h, in methanol, 63℃	84	6.0	1.13	6.8	Copolym.
PNIPAM-1260	- (f)	In DMF	-	10.6	1.18	12.6	Copolym.

Notes: (a). RAFT conditions include the duration time, reaction medium and temperature for one-step RAFT polymerization. Noticeably, the RAFT reaction was slowed down by the addition of RB-MA, likely owing to the polymerization retardation effect of the tertiary amine group in the rhodamine unit. (b). The monomer conversion was gained from ^{1}H NMR spectra. (c). N_n, the number-averaged degree of polymerization, was gained by combining the feed ratio and the monomer conversion for four short PNIPAM samples. N_n is calculated according to the equation $X\times[\text{NIPAM}]_0/[\text{CTA}]_0$, where X is the monomer conversion in RAFT, and $[\text{NIPAM}]_0$ and $[\text{CTA}]_0$ are the initial molar concentrations of NIPAM and CTA, respectively. N, the weight-averaged degree of polymerization, is the product of N_n and PDI. N_n and N of PNIPAM-1260 were gained from the well-defined SEC analysis using a light scattering detector. (d). PDI is short for the polydispersity index defined as the value of M_w/M_n, given by SEC analysis. (e). End-capping and Copolym., short for copolymerization, are the approach 2 and approach 1 in Scheme 1 in the text, respectively. The labeling efficiency of PNIPAM samples is shown in SI-2.7. (f). PNIPAM-1260, was prepared by two successive RAFT steps with different feed ratios and NIPAM conversions.

In order to purify the fluorescent polymers, the 30 mg pink polymer solids dissolved in 1.5 mL aqueous solution and 1.0 mL ethanol was added slowly with strong stirring. The precipitates were collected by centrifugation. Three precipitation steps removed substantially the unreacted fluorescent monomer. The resultant pink PNIPAM was treated sequentially by the centrifugal ultrafiltration (MWCO of 10 000 g·mol^{-1}) in aqueous solution of 0.05 mol·L^{-1} $NaClO_4$, the dialysis in a membrane tube (MWCO of 7 000 g·mol^{-1}) against deionized water and the lyophilization.

2.2 RAFT synthesis of PNIPAM-86 and the labeling at the chain end

The RAFT synthesis of PNIPAM-86 followed the above procedure for synthesizing PNIPAM with other molecular weights but with no addition of the RB-MA comonomer. The as-prepared white solid of PNIPAM-86 was fluorescently labeled in two steps (see Approach 2 of Scheme 1 in text). The carboxyl group of 4.3 mg PNIPAM in 100 μL THF was activated by NHS (2.0 mg) and DCC (1.0 mg) in excess for 0.5 hour at 4 ℃. After adding SulfoRB-NH_2 (1.6 mg, 5 equal amount) in 100 μL DMF solution containing 0.5 μL Et_3N, the reaction was kept for 24 hours at ambient temperature. The reaction mixture was treated sequentially by the column chromatography of polystyrene gel in DMF, the centrifugal ultrafiltration (MWCO of 5 000 $g \cdot mol^{-1}$) in aqueous solution of 0.05 $mol \cdot L^{-1}$ $NaClO_4$, the dialysis in a membrane bag (MWCO of 3 500 $g \cdot mol^{-1}$) against deionized water and the lyophilization.

2.3 Proton nuclear magnetic resonance (^1H NMR) characterization

A small part of the raw RAFT reaction solution was dried and subjected to ^1H NMR (400 MHz, Bruker) analysis in $CDCl_3$. The NIPAM conversion was calculated by comparing the integrated areas of characteristic peaks as the tertiary hydrogen in the isopropyl group had well-separated peaks with the chemical shift at 4.0 ppm and 3.9 ppm for NIPAM monomer and PNIPAM, respectively (see Fig. S1-S5). By combining the feed ratio and the monomer conversion, the number-averaged degree of polymerization (N) was determined as 86, 190, 290 and 680 for the four PNIPAM samples. The ^1H NMR spectra of PNIPAM samples with the peak integrating were plotted via MestReNova (Version 6.1, Mestrelab Research S.L.).

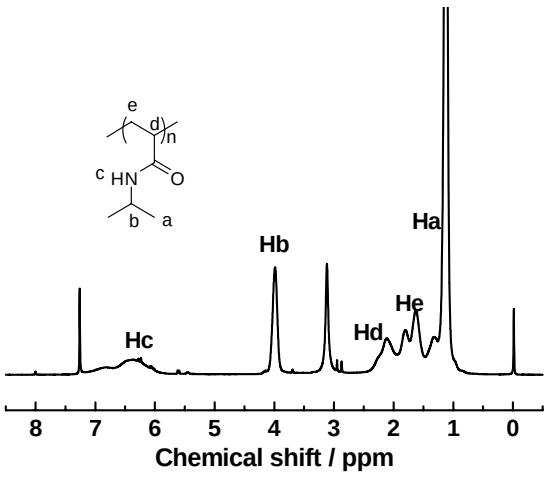

Figure S-1. ^1H NMR spectrum of PNIPAM by RAFT polymerization in $CDCl_3$. The peak with a chemical shift of 3.2 arises from solvent residuals.

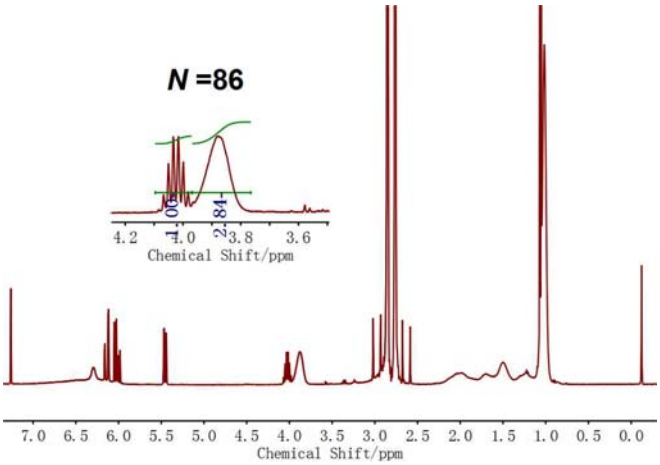

Figure. S-2. ^{1}H NMR spectrum of raw RAFT reaction residues of *N*=86 in $CDCl_3$.

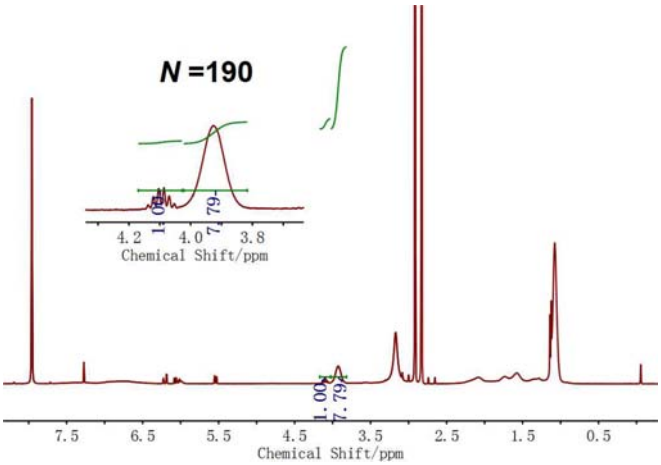

Figure S-3. ^{1}H NMR spectrum of raw RAFT reaction residues of *N*=190 in $CDCl_3$.

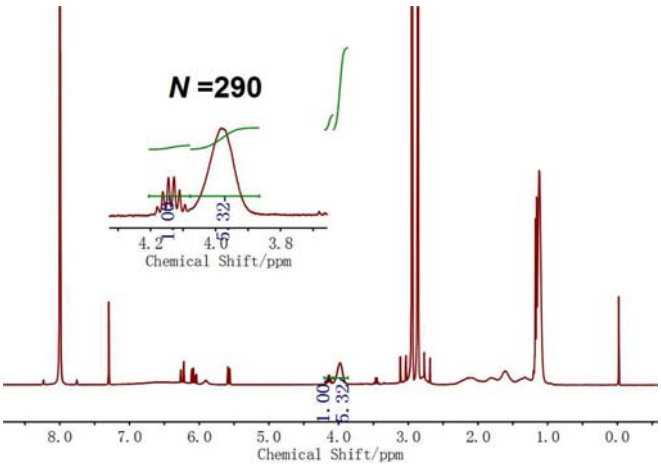

Figure S-4. ^{1}H NMR spectrum of raw RAFT reaction residues of *N*=290 in $CDCl_3$.

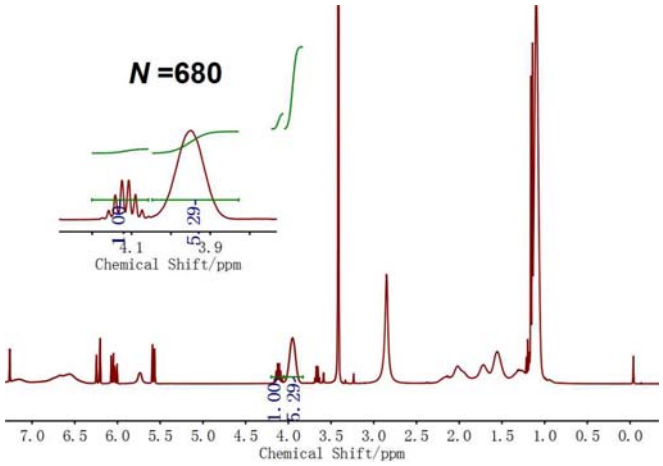

Figure S-5. ^{1}H NMR spectrum of raw RAFT reaction residues of *N*=680 in $CDCl_3$.

2.4 SEC characterization of PNIPAM (N = 86, 190, 290 and 680)

The molecular weight distribution, M_w/M_n, was determined by size exclusion chromatography (SEC; WATERS). DMF containing 0.01 mol·L^{-1} LiBr was used as the eluent with a flow rate of 1.0 mL·min^{-1} at 50 ℃. The SEC system was equipped with a Waters 515 HPLC pump and a combination of three Waters Styragel columns (HT-2, HT-4 and HT-5). The effective molar mass range is 100-10 000, 5 000-600 000 and 50 000-4 000 000 g·mol^{-1}, respectively. Monodisperse polystyrene standards were used to calibrate the SEC system. It used a Rheodyne 7725i sampler and a Waters 2414 refractive-index (RI) detector.

2.5 MALDI-TOF MS characterization of PNIPAM-86

The absolute molecular weight of PNIPAM-86 was confirmed by matrix-assisted laser desorption-ionization time-of-flight mass spectrometry (MALDI-TOF MS). MALDI-TOF MS was conducted on a Bruker BIFLEX III Mass Spectrometer. Tetrafuran was used as the solvent to dissolve PNIPAM. As shown in Fig. S-6, the result is M_n = 8529 g·mol^{-1} (N_n = 75), M_w = 8682 g·mol^{-1} (N = 77) and PDI = 1.02, which is well consistent with the aforementioned result combining the ^{1}H NMR data and the feed ratio of RAFT (N_n = 74 and N = 86 in Table S-1).

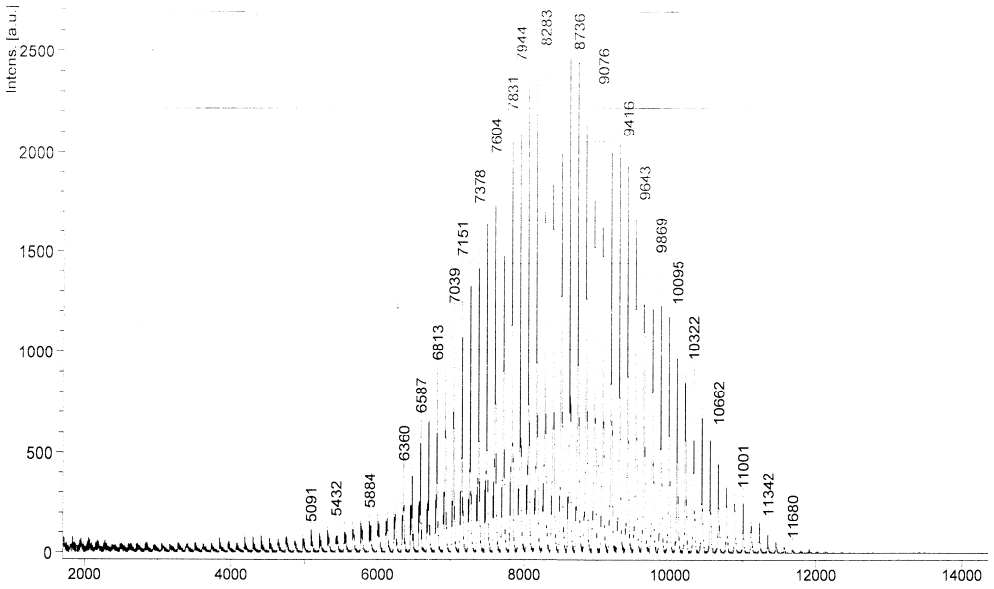

Figure S-6. MALDI-TOF MS spectrum of PNPAM-86. The horizontal axis is the ratio of charge to mass unit (m/z).

2.6 RAFT synthesis of PNIPAM-1260 in two steps with the labeling by copolymerization

It is hard to synthesize PNIPAM with a large *N* and a low polydispersity index (PDI) in one step. Thus PNIPAM with *N*=1260 was prepared in two RAFT steps in a similar way to synthesize a block copolymer. Firstly, RAFT was conducted with the feed ratio of [NIPAM] : [CTA] : [V-501] = 520 : 1 : 0.1. The polymerization was carried out in DMF with vigorous stirring at 65 ℃ under argon atmosphere for 3 hours. The reaction mixture was precipitated into diethyl ether three times and dried under vacuum overnight, producing macromolecular CTA (MacroCTA). The RAFT yield was 70% according to the weighting method and thus *N* of MacroCTA is estimated as 360. In the second step, the red solution with the feed ratio of [NIPAM] : [MacroCTA] : [V-501] : [RB-MA] = 5000 : 1 : 0.1 : 2 in DMF was subjected to reaction at 65 ℃ under argon atmosphere for 11 hours. The red reaction mixture was precipitated into diethyl ether three times and dried by vacuum.

The as-prepared polymer has a PDI of 1.32. Narrowly distributed PNIPAM was obtained after three simple fraction steps. A proper amount of n-hexane was slowly added with strong stirring into the acetone solution of PNIPAM until most polymer species appeared as a pink and viscous precipitate. The precipitate was collected and dried. Three precipitations resulted in PNIPAM with a PDI of 1.18. Any unreacted fluorescent residues were completely removed from PNIPAM in the same procedure as that for the PNIPAM-680 samples.

2.7 SEC characterization of PNIPAM-680 and PNIPAM-1260

A well-defined SEC using a light-scattering detector precisely determined the molecular weight of PNIPAM-1260 under the supervision of qualified scientists. DMF was used as the eluent with a flow rate of 0.5 mL·min^{-1} at 60 ℃. The solution of PNIPAM in DMF was at 5 mg·mL^{-1}. A mixed-bed column (Polymer Labs, PLgel Mixed-C, 300×7.5 mm) was employed at a column temperature of 60 ℃. The signal detector was a Viscotek-TDA (302 RI, viscosity, 90° and 7° true low angle light scattering detectors, and a 7 mW laser with a wavelength of 670 nm). Monodisperse

polystyrene standards were used to calibrate the SEC system. The value of refractive index increment, dn/dc, in DMF at 60 ℃ was adopted as 0.0731mL·g^{-1} in previous publications by McCormick *et al.*[3] As shown in Fig. S-7, the result is $M_n = 1.20\times10^5$ g·mol^{-1}, $M_w = 1.43\times10^5$ g·mol^{-1} and PDI = 1.18. The weight-averaged value $N = 1260$ based on the measured M_w was adopted.

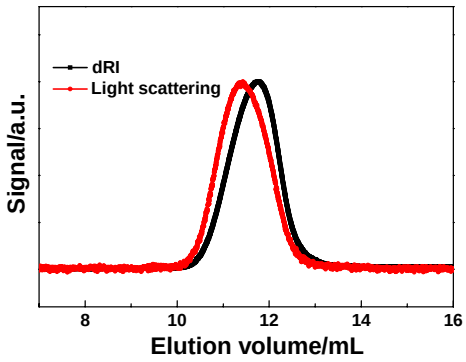

Figure S-7. SEC curve of PNIPAM-1260 with the light scattering signal (red line) and dRI signal (black line). DMF was used as the eluent at 60°C. Characterization was performed in Prof. Taihyun Chang's laboratory (POSTECH).

In addition, the sample of PNIPAM-680 was also subjected to this SEC characterization. As shown in Fig. S-8, the result is $M_n = 6.6\times10^4$ g·mol^{-1} ($N_n = 580$), $M_w = 7.5\times10^4$ g·mol^{-1} ($N = 660$) and PDI = 1.13, which is well consistent with the aforementioned result ($N_n = 600$) combining the ^{1}H NMR data and the feed ratio of RAFT.

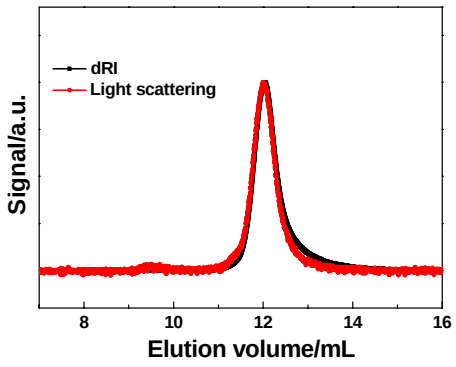

Figure S-8. SEC curve of PNIPAM-680 with the light scattering signal (red line) and dRI signal (black line). DMF was used as the eluent at 60°C. Characterization was performed in Prof. Taihyun Chang's

2.8 Labeling efficiency of PNIPAM

Fluorescence spectra were recorded using a Cary Eclipse fluorescence spectrophotometer (Varian) with an intense Xenon flash lamp as the light source. All emission spectra were recorded at the same slit width and scan speed (600 nm·min^{-1}). Firstly a working curve was plotted which revealed fluorescence intensity at the 569 nm absorbance peak of rhodamine B (RB) in ethanol, I_{569}, as a function of RB concentration, c_{RB}. The linear fitting throughout the low concentration range of the fluorescence dye goes through the origin as I_{569}=1484c_{RB}, where c_{RB} has the unit of 10^{-6} M. The

fluorescence of the ethanol solution of labeled PNIPAM at a certain concentration was examined. Ignoring the insignificant difference of the fluorescence spectrum of the RB unit tagged on PNIPAM from that of free RB molecules, the concentration of the tagged RB unit on PNIPAM chains can be obtained according to the working curve, and the labelling efficiency of PNIPAM was calculated as the ratio of the actual RB concentration to the actual polymer concentration.

For example, 2 mL ethanol solution of 3.5 mg PNIPAM-680 was diluted 8 times so that its fluorescence intensity at 569 nm (609 units) under the same measurement condition fell into the measureable range. According to the working distance the concentration of RB unit in the PNIPAM solution was deduced as 0.41×10^{-6} M. As the actual molar concentration of PNIPAM-680 was 2.8×10^{-6} M, the labeling efficiency of PNIPAM-680 is estimated as 15%. Similarly, the labeling efficiency of PNIPAM-190 and PNIPAM-290 is 56% and 24%, respectively.

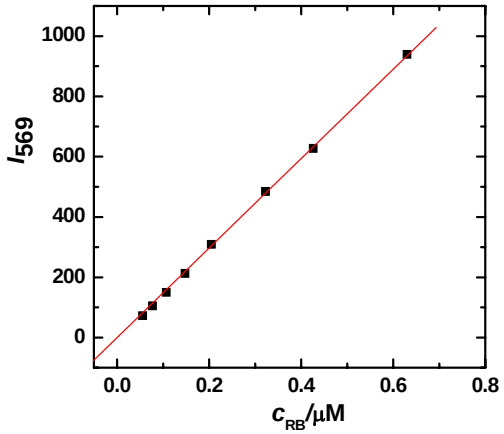

Figure S-9. Fluorescence intensity at the absorbance peak of 569 nm, I_{569}, as a function of rhodamine B (RB) concentration, c_{RB}, in ethanol solution. The linear fitting (solid line) of I_{569} vs. c_{RB} is indicative of no dye quenching within the range of low RB concentration for the working curve.

3. Dynamic laser light scattering (DLS)

The diffusion coefficient of monodisperse fluorescent nanoparticles was measured by a commercial laser light scattering spectrometer (ALV/DLS/SLS-5022F, Germany) with a 22 mW He-Ne laser at 633 nm (Uniphase, USA) as the light source.[4] The sample cell was held in a thermostat, refractive index matching vat filled with purified and dust-free toluene. The sample's temperature was controlled at 25.0°C. Every sample was measured at five scattering angles (30, 60, 90, 120 and 150°). The intensity-intensity correlation function was acquired by an ALV-5000 multi-τ digital time correlator.

Fig. S-10 shows the D values of the fluorescent nanoparticle in the glycerol solution as a function of the concentration of glycerol at 25°C as measured by DLS. The inset shows the plot of the decay rate (Γ) versus the square of the scattering vector (q^2), in which the excellent linearity through the origin indicates the pure Brownian motion of the nanoparticle and the validity of the determination of D values. The values of D decreased with the increase in the glycerol concentration as a result of the continuous increase in the solution viscosity.[5] The hydrodynamic diameter of the fluorescent particle was found to remain constant (107.2 ± 0.6 nm). This value is in agreement with the value of

particle size (0.1 μm) provided by the manufacturer.

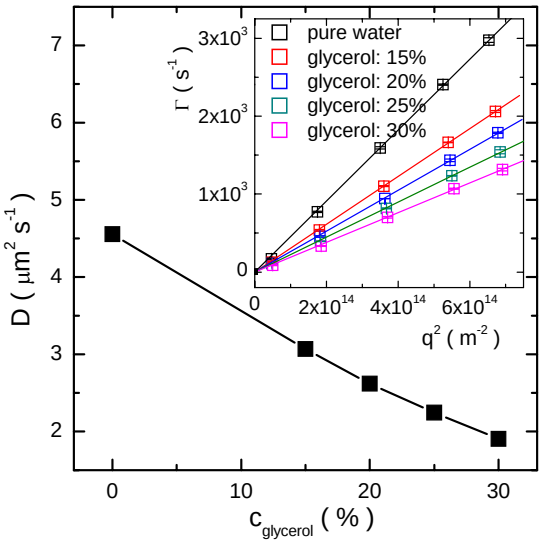

Figure S-10. The value of diffusion coefficient (D) of the fluorescent nanoparticle in glycerol aqueous solution as a function of the concentration of glycerol by weight ($c_{glycerol}$) at 25°C via DLS. Inset: The decay rate (Γ) as a function of the square of the scattering vector (q^2).

4. Fluorescence correlation spectroscopy (FCS)

A home-built single-photon FCS system was based on an inverted IX-71 Olympus microscope. The fluorescence emission was separated from the excitation light using a 525/25 band-pass filter. The fluctuation in the fluorescence signal was measured independently by two single-photon counting modules (Hamamatsu) in a confocal detection geometry. A small pinhole aperture of 60 μm was employed in order to reduce possible optical aberrations. The data acquisition, auto-correlation analysis and photon counting histogram (PCH) were performed on the ISS platform (ISS Inc.). The minimal timing value for auto-correlation analysis was 8 μs to cut off any possible photophysical effect of triplet state. Every adopted D value is an average over at least six measurements in order to gain a precise statistical value. The room temperature for FCS measurements was kept at 20 ℃ or at 25 ℃, depending on the experiments.

The principle of FCS has been reviewed.[6] The critical size parameters of confocal volume of FCS are the radii of the ellipsoid sphere of the light focus in the short and long axial, w_0 and z_0, respectively, as the light intensity decays to $1/e^2$ from the maximum value at the very focus center. According to the equation describing the auto-correlation function $G(\tau)$ in the text, the fitting of auto-correlation curves leads to D values on the assumption that the focal spot assumes a three-dimensionally Gaussian intensity distribution. Experimentally, w_0 was calibrated every time using R6G in aqueous solution with a known D of 366 $\mu m^2 \cdot s^{-1}$ at 20 ℃ or equally 420 $\mu m^2 \cdot s^{-1}$ at 25 ℃. w_0 remained approximately 300 nm with a variation less than 10 nm at low focus depths. A relatively concentrated aqueous solution of R6G (30 nM) in a fresh and hydrophilic cell was employed to estimate z_0 ~1.5 μm, and z_0 was fixed at 1.5 μm during fitting D values because z_0 casts negligile effect on the determination of D of probes.

Fundamental data on the density, viscosity[7] and the refractive index[8] of the water-ethanol

mixtures are shown in Fig. S-11. The ethanol content are denoted as the weight fraction, c_2, and the molar fraction, x_{EtOH}, of ethanol in water-ethanol mixture:

$$c_2 = \frac{m_{EtOH}}{m_{EtOH} + m_{H_2O}}$$

$$x_{EtOH} = \frac{m_{EtOH} / M_{EtOH}}{m_{EtOH} / M_{EtOH} + m_{H_2O} / M_{H_2O}} = \frac{c_2 / M_{EtOH}}{c_2 / M_{EtOH} + (1 - c_2) / M_{H_2O}}$$

where m_{EtOH} and m_{H2O} are the mass of ethanol and water, respectively; M_{EtOH} and M_{H2O} are the molar mass of ethanol and water, respectively.

The change of diffusion coefficient, D, of PNIPAM with c_2 in water-ethanol mixture is plotted, as shown in Fig. S-12. The hydrodynamic radius, R_H, of PNIPAM is related to the diffusion coefficient value by Stokes-Einstein relation.

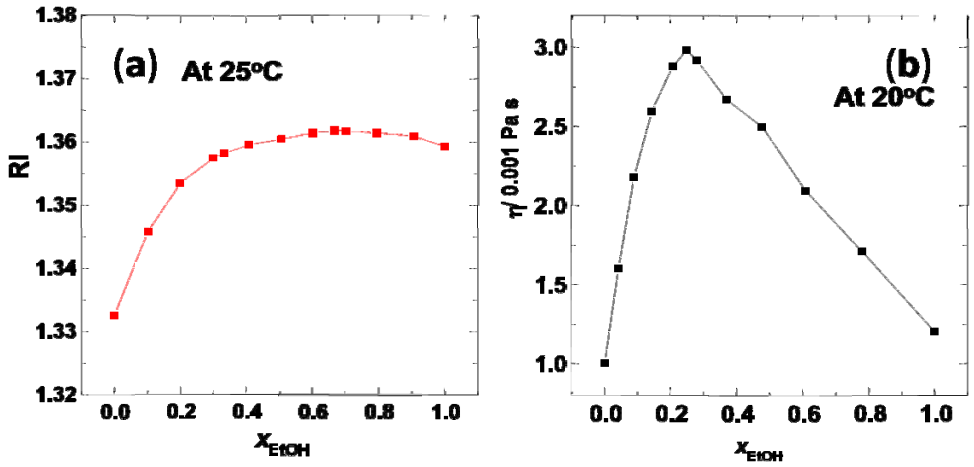

Figure S-11. (**a**). Refractive index (RI) of water-ethanol mixture as a function of the molar fraction of ethanol (x_{EtOH}) at 25°C. [7] (**b**). Viscosity (η) of water-ethanol mixtures as a function of x_{EtOH} at 20°C. [6]

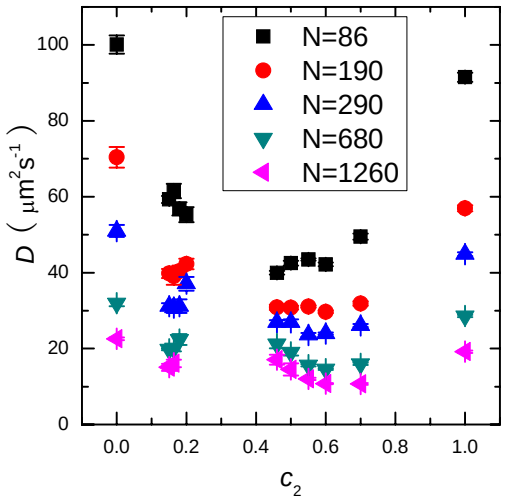

Figure S-12. The diffusion coefficient of PNIPAM (D) as a function of the ethanol fraction by weight (c_2) in water-ethanol mixture. The N values of PNIPAM are indicated.

Moreover, the observed dynamics of single polymer chains can be supported in the following aspects. Firstly, as the used probe concentrations stay at the order of 10^{-9} mol·L^{-1}, the mean distance between two neighboring chains is more than 1 μm (several hundred times of a chain size). Thus our FCS experiments can probe single separated chains. Secondly, the acquired spectra of photon counts in FCS were even without any peaks of photon bursts induced by strongly fluorescent aggregations. Thirdly, the single-component dynamics for polymer diffusion is manifested by well-fitted auto-correlation curves of FCS (Fig. 3 in the text). Fourthly, the photon counting histogram (PCH) acquired simultaneously with FCS gave supportive information on the single chain level, as shown below.

5. Photon counting histogram (PCH)

The PCH analysis and FCS are two methods of fluorescence fluctuation spectroscopy. The PCH captures the amplitude distribution of the fluctuations in the fluorescence intensity.[9] It is capable of characterizing the brightness and concentration of fluorescent particles, and also can resolve heterogeneity arising from different fluorescent species present at the single molecule level.[10] Therefore, the PCH was employed to support the single chain dynamics without clusters or aggregations in our FCS measurements.

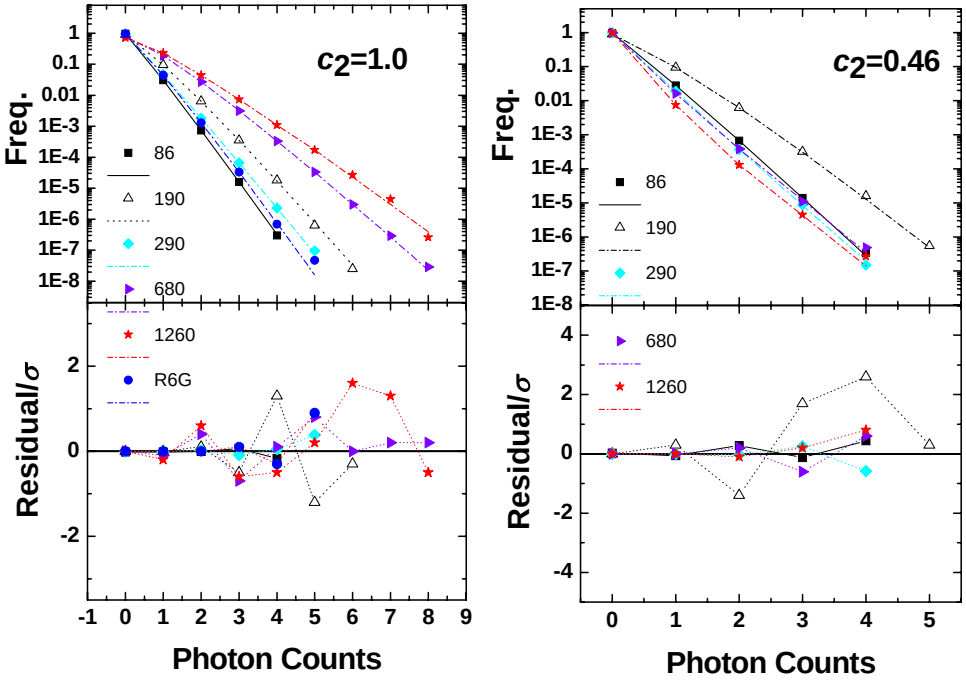

Figure S-13. Experimental PCH plots of five PNIPAM samples (*N* indicated, solid symbols) and the corresponding best fit (dashed dots) of single species with the correction of the observation volume by the one-photon excitation. PNIPAM chains of different chain conformations, random coils at c_2 = 1.0 (**a**) and collapsed globules at c_2 = 0.46 (**b**), are subjected to PCH analysis. R6G in water is also subjected to the PCH analysis. Small residuals in unit of the standard deviation (σ) shown in the lower panels in (**a**) and (**b**) indicate good fitting.

Experimentally, PCH signals were simultaneously acquired with FCS and analyzed on the same platform (ISS Inc.) as FCS. We adopted the fitting procedure with the correction model of the observation volume by the one-photon excitation and the single species fitting provided by ISS platform.[11] As shown in Fig. S-13, experimental data can be well fitted by the super-Poisson distribution, indicating that the dynamics is at the single molecule level. Otherwise, the PCH results cannot be fitted with the assumption of a single component for PNIPAM probes with clusters and/or aggregates, as shown in Fig. S-14.

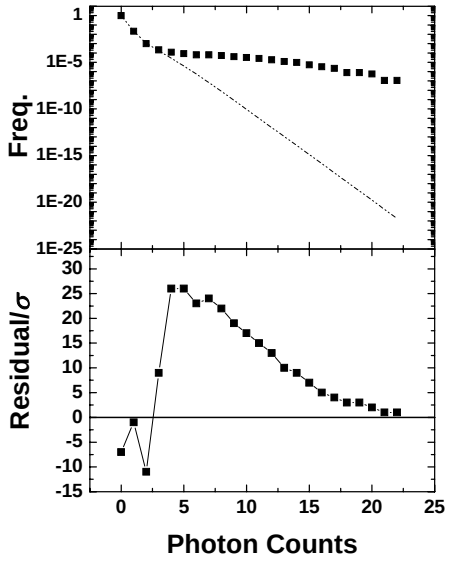

Figure S-14. A typical experimental case of PCH of PNIPAM chains with aggregates (solid symbols) and the corresponding best fit (dashed dots) of single species with the correction of the observation volume by the one-photon excitation at $c_2 = 0.45$. In the precipitation range of the ethanol concentration PNIPAM chains formed clusters and aggregates, and it turned to be impossible to fit the PCH signals. Large and random residuals shown in the lower panels indicate the poor fitting of single species, a result of aggregates present in the sample solution.

6. The fit of the scaling index *v* in the relationship of $R_H \sim N^v$

The values of v at various c_2 values were obtained by the least-square linear fit in Origin (Version 7.5), as shown in Fig. S-15. The v values are plotted against c_2, and then transformed to the plot of v versus x_{EtOH} (see Fig.S-16).

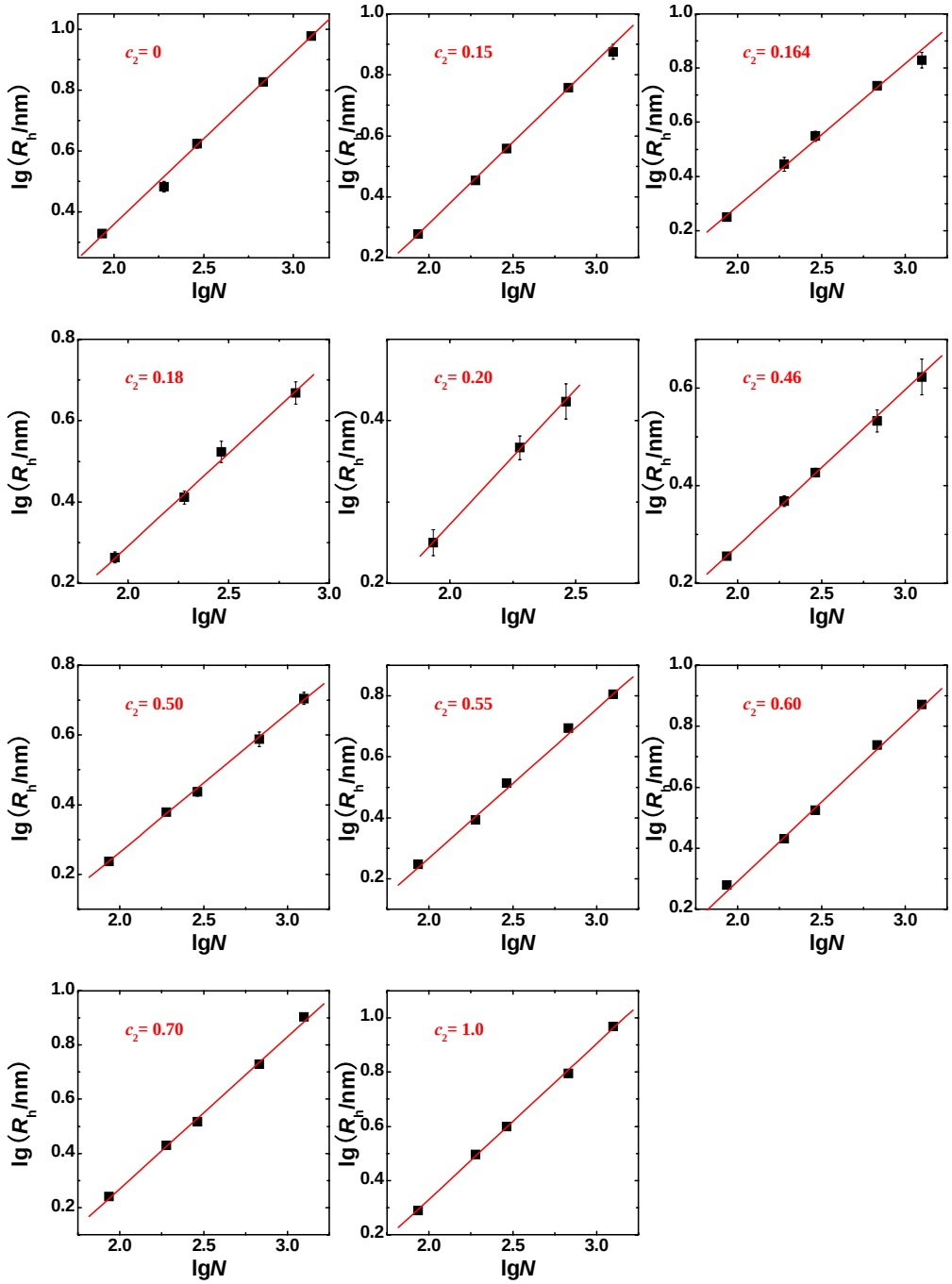

Figure S-15. R_H of PNIPAM as a function of N in the doubly logarithmic plot for various c_2. Error bars are indicated. The slope from a least-square linear fitting is the corresponding scaling index v.

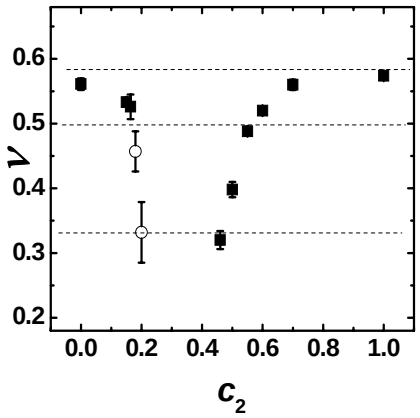

Figure S-16. The scaling exponent v in the relationship of $R_H \sim N^v$ as a function of c_2. All measurements were conducted at 20°C. Horizontal dashed lines respond to the predicted scaling indexes (0.588, 0.5 and 1/3). Error bars are indicated for every data point. The hollow symbols are based on four (c_2=0.18) or three (c_2=0.20) short chains.

7. The fit of scaling indexes using the number-averaged N_n

The values of v were fitted using the number-averaged N_n and plotted against the ethanol concentration c_2. No distinct difference from scaling laws using the weight-averaged N was observed.

References

1. Shi, Y.; Liu, G.; Gao, H.; Lu, L.; Cai, Y. *Macromolecules* **2009,** 42, (12), 3917-3926.
2. Lai, J. T.; Filla, D.; Shea, R. *Macromolecules* **2002,** 35, (18), 6754-6756.
3. Convertine, A. J.; Ayres, N.; Scales, C. W.; Lowe, A. B.; McCormick, C. L. *Biomacromolecules* **2004,** 5, (4), 1177-1180.
4. Hao, J.; Cheng, H.; Butler, P.; Zhang, L.; Han, C. C. *J. Chem. Phys.* **2010,** 132, (15), 154902.
5. Sheely, M. L. *Ind. Eng. Chem. Res.* **1932,** 24, (9), 1060-1064.
6. Oleg, K.; Grégoire, B. *Rep. Prog. Phys.* **2002,** 65, (2), 251.
7. Belda, R.; Herraez, J. V.; Diez, O. *Phys. Chem. Liq.* **2004,** 42, (5), 467-479.
8. Herráez, J.; Belda, R. *J. Solution Chem.* **2006,** 35, (9), 1315-1328.
9. Chen, Y.; Müller, J. D.; So, P. T. C.; Gratton, E. *Biophys. J.* **1999,** 77, (1), 553-567.
10. Müller, J. D.; Chen, Y.; Gratton, E. *Biophys. J.* **2000,** 78, (1), 474-486.
11. Huang, B.; Perroud, T. D.; Zare, R. N. *ChemPhysChem* **2004,** 5, (10), 1523-1531.